

Differential interaction of dicarboxylates with human sodium-dicarboxylate cotransporter 3 and organic anion transporters 1 and 3

Marcel Kaufhold, Katharina Schulz, Davorka Breljak, Shivangi Gupta, Maja Henjakovic, Wolfgang Krick, Yohannes Hagos, Ivan Sabolic, Birgitta C. Burckhardt and Gerhard Burckhardt

Am J Physiol Renal Physiol 301:F1026-F1034, 2011. First published 24 August 2011;
doi:10.1152/ajprenal.00169.2011

You might find this additional info useful...

This article cites 38 articles, 24 of which can be accessed free at:

<http://ajprenal.physiology.org/content/301/5/F1026.full.html#ref-list-1>

Updated information and services including high resolution figures, can be found at:

<http://ajprenal.physiology.org/content/301/5/F1026.full.html>

Additional material and information about *AJP - Renal Physiology* can be found at:

<http://www.the-aps.org/publications/ajprenal>

This information is current as of November 8, 2011.

Differential interaction of dicarboxylates with human sodium-dicarboxylate cotransporter 3 and organic anion transporters 1 and 3

Marcel Kaufhold,¹ Katharina Schulz,¹ Davorka Breljak,² Shivangi Gupta,¹ Maja Henjakovic,¹ Wolfgang Krick,¹ Yohannes Hagos,¹ Ivan Sabolic,² Birgitta C. Burckhardt,¹ and Gerhard Burckhardt¹

¹Abteilung Vegetative Physiologie und Pathophysiologie, Universitätsmedizin Göttingen, Göttingen, Germany; and ²Unit of Molecular Toxicology, Institute for Medical Research and Occupational Health, Zagreb, Croatia

Submitted 25 March 2011; accepted in final form 23 August 2011

Kaufhold M, Schulz K, Breljak D, Gupta S, Henjakovic M, Krick W, Hagos Y, Sabolic I, Burckhardt BC, Burckhardt G. Differential interaction of dicarboxylates with human sodium-dicarboxylate cotransporter 3 and organic anion transporters 1 and 3. *Am J Physiol Renal Physiol* 301: F1026–F1034, 2011. First published August 24, 2011; doi:10.1152/ajprenal.00169.2011.—Organic anions are taken up from the blood into proximal tubule cells by organic anion transporters 1 and 3 (OAT1 and OAT3) in exchange for dicarboxylates. The released dicarboxylates are recycled by the sodium dicarboxylate cotransporter 3 (NaDC3). In this study, we tested the substrate specificities of human NaDC3, OAT1, and OAT3 to identify those dicarboxylates for which the three cooperating transporters have common high affinities. All transporters were stably expressed in HEK293 cells, and extracellularly added dicarboxylates were used as inhibitors of [¹⁴C]succinate (NaDC3), *p*-[³H]aminohippurate (OAT1), or [³H]estrone-3-sulfate (OAT3) uptake. Human NaDC3 was stably expressed as proven by immunochemical methods and by sodium-dependent uptake of succinate ($K_{0.5}$ for sodium activation, 44.6 mM; Hill coefficient, 2.1; K_m for succinate, 18 μ M). NaDC3 was best inhibited by succinate (IC_{50} 25.5 μ M) and less by α -ketoglutarate (IC_{50} 69.2 μ M) and fumarate (IC_{50} 95.2 μ M). Dicarboxylates with longer carbon backbones (adipate, pimelate, suberate) had low or no affinity for NaDC3. OAT1 exhibited the highest affinity for glutarate, α -ketoglutarate, and adipate (IC_{50} between 3.3 and 6.2 μ M), followed by pimelate (18.6 μ M) and suberate (19.3 μ M). The affinity of OAT1 to succinate and fumarate was low. OAT3 showed the same dicarboxylate selectivity with \sim 13-fold higher IC_{50} values compared with OAT1. The data 1) reveal α -ketoglutarate as a common high-affinity substrate of NaDC3, OAT1, and OAT3 and 2) suggest potentially similar molecular structures of the binding sites in OAT1 and OAT3 for dicarboxylates.

EFFICIENT EXCRETION OF ANIONIC endogenous waste products and exogenous compounds including drugs and toxins is an important task of the kidneys. Many organic anions (OA) undergo active *trans*-cellular secretion in renal proximal tubules, involving OA uptake across the basolateral membrane and OA release across the luminal membrane of proximal tubule cells. The uptake of OA from blood across the basolateral membrane into tubule cells is remarkable in several ways. First, OA uptake is considered the rate-limiting step in secretion; second, the uptake occurs against an opposing intracellular negative membrane potential difference; third, a multitude of chemically different OA is accepted as substrates for secretion (8, 30, 36). The mechanism by which OA overcome the opposing driving force during basolateral uptake was clarified in studies

with basolateral membrane vesicles isolated from rat kidneys. Shimada et al. (29) and Pritchard (25) suggested the cooperation of two transporters: a sodium-driven dicarboxylate cotransporter and an OA/dicarboxylate exchanger.

As regards the molecular identity of these cooperating transporters, the sodium-dicarboxylate cotransporter 3 (NaDC3, SLC13A3) takes up dicarboxylates into the cells and thus provides substrates for exchange against extracellular OA through the organic anion transporters 1 and 3 (OAT1, SLC22A6; and OAT3, SLC22A8). NaDC3 was cloned from human, rat, mouse, and winter flounder and found to be expressed in kidneys, liver, placenta, and brain (20). NaDC3 has a high affinity for succinate and α -ketoglutarate, and it translocates three sodium ions with a divalent dicarboxylate, leading to inward currents during uptake (9, 21, 31). OAT1 was cloned from human, monkey, pig, rabbit, rat, and mouse. Expression of OAT1 occurred mainly in kidneys where it is located in the basolateral membrane of proximal tubule cells (8, 30, 36). Cloned OAT1 interacted with numerous drugs and toxins, revealing its importance for renal excretion of xenobiotics (8, 30, 36). The closely related OAT3 was cloned from human, monkey, pig, rabbit, rat, and mouse. In all species, OAT3 expression was highest in the kidneys and it was localized to the basolateral membrane of proximal tubules. Heterologously expressed OAT3 showed a wide substrate specificity overlapping with that of OAT1 (8, 30, 36). The differential contribution of OAT1 and OAT3 to renal OA secretion has been elucidated with knockout mice (12, 32, 35, 37).

Earlier studies with rat renal proximal tubules *in vivo* revealed dicarboxylates as inhibitors of the basolateral uptake of a prototypic OA, *p*-aminohippurate (PAH) (33). Thereby, dicarboxylates with a backbone of at least five carbons exhibited a high affinity for the so-called PAH system. Since, as it became known later, at least two transporters contributed to PAH uptake in these *in vivo* studies, it is not clear whether the observed dicarboxylate specificity can be attributed to OAT1 or OAT3 or to both. Cloned rat OAT1 (34) and OAT3 (1) were inhibited by dicarboxylates with a similar dependence on the number of backbone carbons as reported by Ullrich et al. (33), but quantitative data (IC_{50} or K_i values) were not provided. Mouse OAT1 was best inhibited by glutarate (K_i 6.7 μ M) and adipate (6.4 μ M), weaker by suberate (34.1 μ M), and weakest by fumarate [610 μ M (15)]. As regards human OAT1, interaction with several dicarboxylates was reported, but IC_{50} values were provided only for glutarate [4.9 μ M (10) or 38.3 μ M (17)].

Effective cooperation of NaDC3 and OAT1/OAT3 requires the presence of dicarboxylates accepted with high affinity by

Address for reprint requests and other correspondence: G. Burckhardt, Abteilung Vegetative Physiologie und Pathophysiologie, Universitätsmedizin Göttingen, Humboldtallee 23, 37073 Göttingen, Germany (e-mail: gerhard.burckhardt@med.uni-goettingen.de).

all three transporters. The aim of this study was to provide quantitative data for the interaction of dicarboxylates with human NaDC3, OAT1, and OAT3. To allow for direct comparison of IC_{50} values, all transporters were stably transfected in HEK293 cells. Whereas HEK-OAT1 and HEK-OAT3 cells were previously established (3), we describe here the stable expression of human NaDC3 in HEK cells. We then compared the IC_{50} values for a series of dicarboxylates on NaDC3, OAT1, and OAT3 and found that the C5 dicarboxylate α -ketoglutarate is most suited for the cooperative action of these transporters. The dependence of apparent affinity of NaDC3 on the length of aliphatic dicarboxylates is different from that of OAT1 and OAT3, suggesting binding sites of different substrate recognition properties. A similar preference by OAT1 and OAT3 for dicarboxylates of different lengths, on the other side, indicates closely related substrate binding sites, albeit with different accessibilities.

MATERIALS AND METHODS

Transfected cells. Human NaDC3, OAT1, and OAT3 (GeneBank accession numbers: AF154121, AF097490, and BI760120, respectively) were obtained from Resource Center for Genome Research (RZPD, Berlin, Germany). Stably transfected human epithelial kidney cells T-REX-HEK293-hOAT1, -HEK293-hOAT3, and -HEK293-NaDC3 were established by using the Flp-In expression system (Invitrogen, Darmstadt, Germany) as previously described (3). Cells were selected by hygromycin (10 μ g/ml) and grown in flasks in high-glucose DMEM medium (Invitrogen) supplemented with 10% fetal calf serum (Invitrogen), 1% penicillin/streptomycin, and blastididine (5 mg/l; all antibiotics from Sigma, Deisenhofen, Germany). Control cells were transfected with the vector alone. Cultures were seeded at a density of 2×10^5 cells/well and maintained in humidified atmosphere that contained 5% CO_2 at 37°C.

Solutions. A standard mammalian Ringer solution (MRi) was used for the uptake experiments. MRi contained (in mM) 130 NaCl, 4 KCl, 1 $CaCl_2$, 1 $MgSO_4$, 1 NaH_2PO_4 , 20 HEPES, and 18 glucose at pH 7.4. Dicarboxylates were added at various concentrations to determine the IC_{50} values. Nominal sodium-free conditions were obtained by replacing NaCl by *N*-methyl-D-glucamine chloride. Chemicals were purchased from Sigma or Applichem (Darmstadt, Germany) and were of analytical grade.

Antibodies. The immune serum against human NaDC3 was raised in rabbits against the synthetic peptide (ARAVIREEYQNLGPIK), corresponding to 16 amino acids of the internal region of NaDC3 (Eurogentec, Seraing, Belgium). Peptide-specific antibodies (NaDC3-Ab) were affinity purified from the immune serum on an affinity column. The specificity of NaDC3-Ab was analyzed by Western blotting of total cell membranes isolated from the NaDC3 stably transfected HEK293 cells, and by immunocytochemistry of the same cells. The vector-transfected HEK293 cells were used as a negative control. The secondary antibodies, i.e., the CY3-labeled (GARCY3) and alkaline phosphatase-labeled (GARAP) goat anti-rabbit IgG, were purchased from Jackson Immuno Research Laboratories (West Grove, PA).

Immunocytochemistry. The vector-transfected (control cells) and NaDC3-transfected HEK293 cells were grown on coverslips in 24-well plates (Sarstedt, Nümbrecht, Germany). While still in wells, the cells were fixed with 4% *p*-formaldehyde (in PBS) for 30 min. The fixative was removed by suction, and the cells were rinsed with four abundant changes of PBS. The cells were then covered with 10 mM citrate buffer, pH 3, and heated in a microwave oven for 20 min at 800 W (4 cycles, 5 min each) to retrieve the antibody-binding sites. After cooling down for 20 min at room temperature in the same buffer, the cells were rinsed with PBS (3 times 5 min) and used in immunostain-

ing procedure, as described in detail for our recent study of OAT2 expression in rat and mouse kidneys (18). Briefly, following blocking with 1% bovine serum albumin (in PBS) for 30 min, the cells were incubated with NaDC3-Ab (dilution 1:150) at 4°C overnight, rinsed, incubated with GARCY3 (1.6 μ g/ml) for 60 min at room temperature, and rinsed again. The coverslip with the cells was then transferred on a microscope slide, overlaid with the fluorescence fading retardant Vectashield (Vector Laboratories, Burlingame, CA), veiled with a larger coverslip, and sealed with a nail polish. To test the staining specificity with the NaDC3-Ab, the cells were 1) stained with the primary antibody that had been blocked with the immunizing peptide (final concentration 0.5 mg/ml) for 4 h at room temperature before use in immunocytochemistry and 2) stained only with the secondary antibody (the primary antibody was omitted). The immunostaining was examined with an Opton III RS fluorescence microscope (Opton Feintechnik, Oberkochen, Germany) and photographed using a Spot RT Slider digital camera and software (Diagnostic Instruments, Sterling Heights, MI). The photos were imported into Adobe Photoshop 6.0 software for processing, assembling, and labeling. The same software was used for conversion of the CY3-related red fluorescence into black and white mode.

Preparation of total cell membranes, SDS-PAGE, and Western blotting. Cells grown in 150-mm disks were harvested, dispersed, and homogenized in ice-cold PBS by sonication. The homogenate was centrifuged at 6,000 *g* for 10 min. The pellet was discarded, and the supernatant was centrifuged at 150,000 *g* for 30 min. The resulting pellet was dispersed in PBS, the protein was measured by the Bradford assay (5), and the sample underwent SDS-PAGE and Western blotting as described in detail previously (18). Briefly, total cell membranes (TCM) were mixed with nonreducing Laemmli buffer and denatured at 65°C for 15 min. Proteins were separated through 10% SDS-PAGE mini gels, and then electrophoretically wet-transferred to an Immobilon membrane (Millipore, Bedford, MA). The membrane was then blocked in blotto-buffer (5% nonfat dry milk, 0.15 M NaCl, 1% Triton X-100, 20 mM Tris-HCl, pH 7.4) for 1 h, incubated in the blotto-buffer containing the NaDC3-Ab (1:200) at 4°C overnight, rinsed, incubated at room temperature with GARAP (0.1 μ g/ml) for 60 min, rinsed, and the protein bands were visualized by the alkaline phosphatase activity-mediated reaction using 5-bromo-4-chloro-3-indolyl phosphate (1.65 mg/ml) and nitro blue tetrazolium (3.3 mg/ml) as indicators.

To show specific labeling, the NaDC3-Ab was preincubated with the immunizing peptide (final concentration, 0.5 mg/ml) for 4 h at room temperature before use in Western blotting. The relative molecular mass (M_r) of the labeled protein bands was estimated by using Protein Ladders (Fermentas, Ontario, Canada) as markers.

Deglycosylation assay. TCM isolated from the NaDC3-transfected HEK293 cells were incubated with the enzyme peptide-*N*-glycosidase F (PNGase F; Roche, Mannheim, Germany) according to the manufacturer's recommendations. The reaction mixture in a total volume of 20 μ l contained 16 units of PNGase F and 60 μ g TCM protein from the NaDC3-transfected cells. In the control sample, distilled water was substituted for PNGase F. The reaction was carried out for 1 h at 37°C. Thereafter, the samples underwent SDS-PAGE and Western blotting, as described above.

Tracer uptake experiments. NaDC3-, OAT1-, OAT3-, and vector-transfected HEK293 cells were harvested and plated into 24-well plastic dishes (Sarstedt) at a density of 2×10^5 cells/well. Transport assays were performed 48 h after the cells were seeded in MRi. Cells were washed twice with 0.5 ml MRi and incubated for the time indicated in the Table 1 or figure legends in MRi that contained 1 μ M [^{14}C]succinate for NaDC3, 1.1 μ M PAH for hOAT1, and 10 nM [3H]estrone sulfate (ES) for hOAT3, respectively. The specific activities of the labeled compounds were 58 mCi/mmol [^{14}C]succinate, 4.35 Ci/mmol [3H]PAH, and 57.3 Ci/mmol [3H]ES, respectively (all labeled substances were from Perkin Elmer, Rodgau, Germany). In all experiments, uptake was terminated by removal of the radioactive

Table 1. Influence of various dicarboxylates on the uptake of succinate, PAH, and ES in NaDC3-, OAT1-, and OAT3-transfected HEK293 cells

Substance	IC ₅₀ (μM) for NaDC3-Mediated Succinate Uptake	n	IC ₅₀ (μM) for OAT1-Mediated PAH Uptake	n	IC ₅₀ (μM) for OAT3-Mediated ES Uptake	n
Malonate	no inhibition	2	no inhibition	3	no inhibition	3
Maleate	no inhibition	2	12,950 ± 1,258	4	141,100 ± 86,300	3
Fumarate	95.2 ± 13.9	2	1,733 ± 353	3	21,100 ± 2,800	3
Succinate	23.5 ± 6.6	2	4,825 ± 680	4	55,700 ± 16,500	3
Glutarate	138 ± 6.5	3	3.3 ± 1.2	4	78.5 ± 5.3	4
α-Ketoglutarate	69.2 ± 8.2	3	4.7 ± 1.2	4	92.8 ± 33.6	4
Adipate	1,140 ± 70.7	2	6.2 ± 1.0	5	136 ± 57	3
Pimelate	9,450 ± 2,050	2	18.6 ± 2.6	3	634 ± 225	4
Suberate	no inhibition	2	19.3 ± 2.2	3	232 ± 42	3

Results are means ± SE of *n* independent cell preparations. Influence of various dicarboxylates on the uptake of succinate, *p*-aminohippurate (PAH), and estrone sulfate (ES) in NaDC3-, organic anion transporter 1 (OAT1)-, and OAT3-transfected HEK293 cells. Transfected cells were incubated for 5 min in mammalian Ringer (MRi) containing 1 μM [¹⁴C]succinate or for 1 min in MRi containing either 1.1 μM [³H]PAH (OAT1) or 10 nM [³H]ES (OAT3) as well as increasing concentrations of the respective dicarboxylate. No inhibition, uptake of succinate, PAH, or ES was <10% inhibited by the highest concentration of the respective compound.

medium and immediate three 0.75-ml washes with ice-cold MRi. The cells were dissolved in 0.25 ml 1 N NaOH by gently shaking for 30 min followed by neutralization with 0.25 ml 1 N HCl. The ³H and ¹⁴C content was determined by liquid scintillation counting (Tricarb 2900TR, Perkin Elmer).

Statistics. The numeric data presented are means ± SE of the number of cell preparations indicated in the table and figure legends. The kinetic parameters, *K_m* and *V_{max}*, for the uptake of succinate by NaDC3-transfected HEK293 cells were calculated by the equation $V = V_{max} \times S^h / (K_m^h + S^h)$, where *V* is the observed uptake at a distinct substrate concentration, *V_{max}* is the maximal uptake of the substrate, *K_m* the Michaelis-Menten constant, *S* the substrate concentration, and *h* the Hill coefficient. The IC₅₀ for the inhibition of the prototypical substrates by various dicarboxylates was calculated by the equation $V_1 = V_0 / (1 + [I]/IC_{50})$, where *V₁* is the transport rate in the presence, *V₀* in the absence of the inhibitor, and [*I*] the concentration of the inhibitor, respectively (adapted from Ref. 11). For [*I*] = IC₅₀, *V₁* becomes half of *V₀*. For all kinetic experiments, the uptake into vector-transfected HEK293 cells was subtracted to obtain transporter-specific uptake. *K_m*, Hill coefficient (see Fig. 2), IC₅₀ values (Table 1), and the linear regression (see Fig. 7) were calculated using the SigmaPlot10 software (Systat, Point Richmond, CA).

RESULTS

Immunochemical characterization of the NaDC3-transfected HEK293 cells. The NaDC3-transfected cells were characterized by immunocytochemistry and Western blotting using the NaDC3-Ab. As shown in Fig. 1A, the antibody stained the plasma membranes and the intracellular domain beneath the plasma membrane (NaDC3-transfected cells, Ab, and inset). This staining was absent following preincubation of the NaDC3-Ab with the immunizing peptide (Fig. 1A, NaDC3-transfected cells, Ab+P) and in the vector-transfected cells (Control cells, Ab). In Western blots of TCM isolated from control cells, no prominent protein band was labeled with the anti-NaDC3 antibody (Fig. 1B, Control, Ab), whereas, in TCM from the NaDC3-transfected cells, the antibody labeled two unsharp protein bands of ~85 and 55 kDa (Fig. 1B, NaDC3, Ab). These bands were absent with the peptide-blocked antibody (Fig. 1B, NaDC3, Ab+P). Since the two labeled bands may represent differentially glycosylated forms of NaDC3, TCM proteins from the NaDC3-transfected cells were deglycosylated with PNGase F, then separated by SDS-PAGE, and subsequently subjected to Western blotting using the anti-

NaDC3 antibody (Fig. 1C). Following incubation without the enzyme, the control sample exhibited the expected two protein bands labeled with the NaDC3-Ab (-PNGase F). However, following the enzymatic digestion (+PNGase F), the upper ~85-kDa band was absent, and the antibody labeled two sharper protein bands of ~48 and ~56 kDa.

Functional characterization of NaDC3-transfected HEK293 cells. Succinate, the prototypical substrate of NaDC3, was used to demonstrate time-dependent uptake of [¹⁴C]succinate in

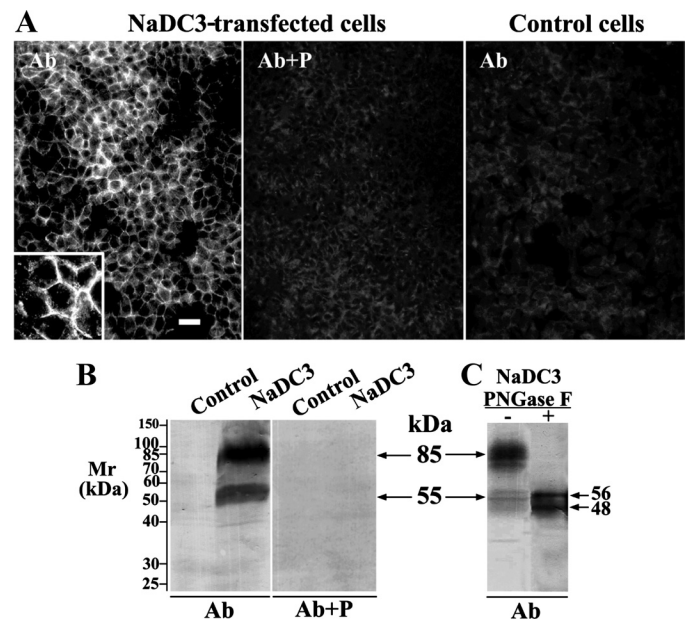


Fig. 1. Immunocytochemical characterization of HEK293 cells stably transfected with human NaDC3. **A:** plasma membrane and the submembrane region of the NaDC3-transfected cells were brightly stained with the NaDC3-Ab (Ab, inset). This staining was blocked by the immunizing peptide (Ab+P). The vector-transfected cells (control cells) remained unstained with the NaDC3-Ab. Bar = 20 μm. **B:** In Western blot of total cell membranes (TCM) from the NaDC3-transfected cells, the NaDC3-Ab labeled 2 protein bands of ~55 and ~85 kDa (Ab), which were absent after preincubating the antibody with the immunizing peptide (Ab+P). Each lane contained 80 μg protein. **C:** In nondeglycosylated TCM, the NaDC3-Ab labeled 2 protein bands, a weaker of ~55 kDa and a stronger of ~85 kDa (-PNGase F), whereas in the PNGase F-treated TCM, the labeled were 2 sharper protein bands of ~56 and ~48 kDa (+PNGase F). Each lane contained 60 μg protein.

NaDC3-transfected cells (Fig. 2A). Uptake of succinate increased with time, and virtually no succinate uptake was detected in vector-transfected cells over this time. To approach initial rate conditions, all further experiments were performed using an incubation time of 5 min. In NaDC3-transfected cells,

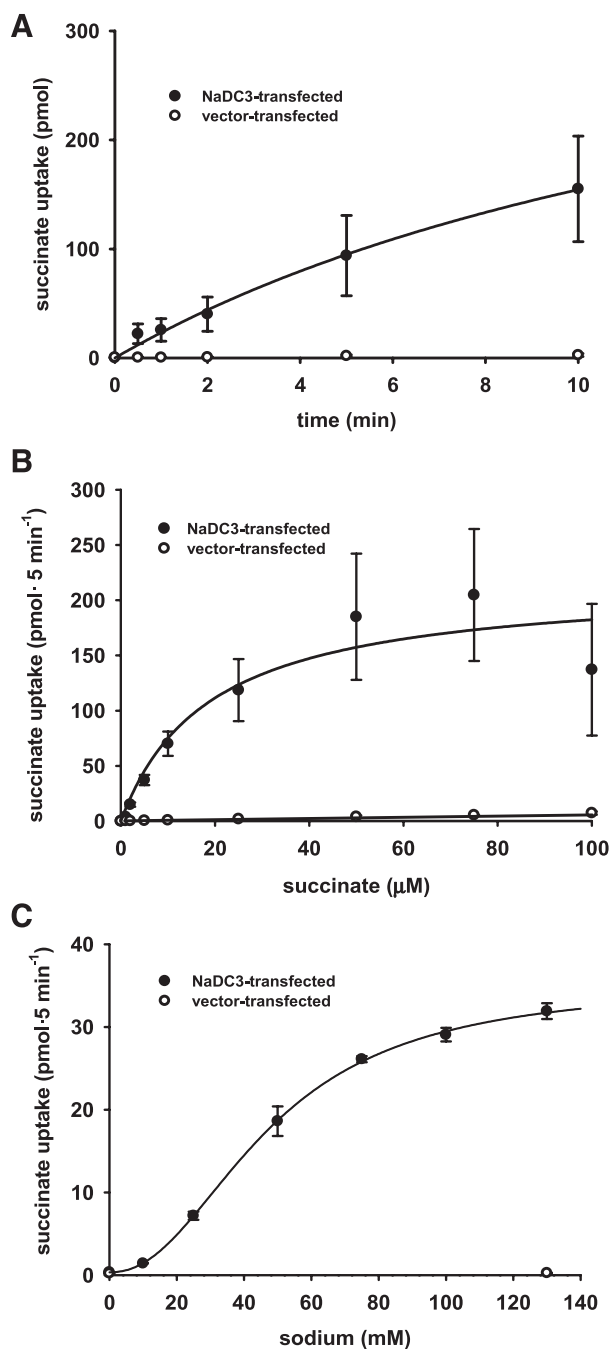


Fig. 2. Time and concentration dependence of succinate uptake into NaDC3-transfected HEK293 cells. A: NaDC3-transfected HEK293 cells (●) and vector-transfected cells (○) were incubated for the times indicated with 1 μM [^{14}C]succinate. B: K_m and V_{max} were determined by incubation of NaDC3-transfected HEK293 cells and vector-transfected cells for 5 min at the indicated succinate concentrations. The concentration of labeled succinate was 1 μM and unlabeled succinate was added to reach the final succinate concentration. C: sodium was varied at the expense of *N*-methyl-D-glucamine to reach the appropriate sodium concentrations at a concentration of labeled succinate of 1 μM . Values are means per well \pm SE of 3–4 preparations.

succinate uptake saturated at succinate concentrations $>50 \mu\text{M}$ (Fig. 2B), revealing a K_m of $18.0 \pm 8.8 \mu\text{M}$ and a V_{max} of $208.0 \pm 31.5 \text{ pmol} \cdot 5 \text{ min}^{-1} \cdot \text{well}^{-1}$. Uptake of succinate into vector-transfected cells was, even at succinate concentrations exceeding 50 μM , negligible. Succinate uptake was sodium-dependent and showed a sigmoidal activation with a Hill coefficient of 2.1 ± 0.9 . Half maximal activation of succinate uptake by sodium occurred at a sodium concentration of $44.6 \pm 2.5 \text{ mM}$ (Fig. 2C).

Comparison of the dicarboxylate specificities of NaDC3-, OAT1-, and OAT3-transfected HEK293 cells. The chemical structures of the dicarboxylates used in this study are provided in Fig. 3. To determine the IC_{50} values, uptake of [^{14}C]succinate, [^3H]PAH, or [^3H]ES into HEK293 cells expressing NaDC3, OAT1, or OAT3, respectively, was measured in the presence of increasing concentrations of dicarboxylates. Figure 4 shows the results for the five-carbon dicarboxylates α -ketoglutarate and glutarate. In these representative experiments on NaDC3 (Fig. 4A), α -ketoglutarate and glutarate inhibited succinate uptake by NaDC3 with IC_{50} values of 69 and 138 μM , respectively. OAT1 was half-maximally inhibited by 5.8 μM α -ketoglutarate and 3.6 μM glutarate (Fig. 4B), and OAT3 by 117 μM α -ketoglutarate and 88 μM glutarate (Fig. 4C), respectively.

The IC_{50} values for all tested dicarboxylates are compiled in Table 1. [^{14}C]Succinate uptake into NaDC3-transfected HEK293 cells was best inhibited by succinate itself. The IC_{50} values increased in the following order: succinate $<$ α -ketoglutarate $<$ fumarate $<$ glutarate $<$ adipate $<$ pimelate. Malonate, maleate, and suberate up to a concentration of 20 mM did not show any inhibition of succinate uptake. α -Ketoglutarate, glutarate, and adipate inhibited PAH uptake into OAT1-transfected HEK293 cells with IC_{50} values below 10 μM , and ES uptake into OAT3-transfected HEK293 cells with IC_{50} values below 140 μM , respectively. Succinate, fumarate, and maleate inhibited marginally, and malonate not at all the uptake of PAH and ES. Dicarboxylates with longer carbon backbones such as pimelate and suberate exhibited IC_{50} values of $\sim 20 \mu\text{M}$ on OAT1 and $< 650 \mu\text{M}$ on OAT3, respectively.

Correlation of the chain length with the inhibitory potency. For easier visualization of the data presented in Table 1, we plotted the $\log \text{IC}_{50}$ against the chain length of the dicarboxylates (Fig. 5). For NaDC3 (▼), $\log \text{IC}_{50}$ steadily increased from succinate (4 carbons) to pimelate (7 carbons). Suberate (8 carbons) did not inhibit succinate uptake in NaDC3-transfected HEK293 cells and is not included. For OAT1 (●) and OAT3 (○), $\log \text{IC}_{50}$ values changed in parallel. Values sharply declined from succinate to glutarate and increased again at longer chain lengths.

No significant correlation was observed in double-logarithmic plots of IC_{50} values for succinate uptake into NaDC3-transfected HEK293 cells against those for PAH uptake in OAT1- (Fig. 6A) or for ES uptake in OAT3 (Fig. 6B)-transfected HEK293 cells: the r^2 values were 0.21 and 0.15 for NaDC3/OAT1 and NaDC3/OAT3, respectively. For NaDC3/OAT1 as well as for NaDC3/OAT3, α -ketoglutarate and glutarate were identified as the best common inhibitors. A double-logarithmic plot of the IC_{50} values with OAT1- and OAT3-transfected HEK293 cells revealed a linear correlation (r^2 0.99; Fig. 7). The regression line has a slightly smaller slope (0.91) than unity and has an intercept of 1.13,

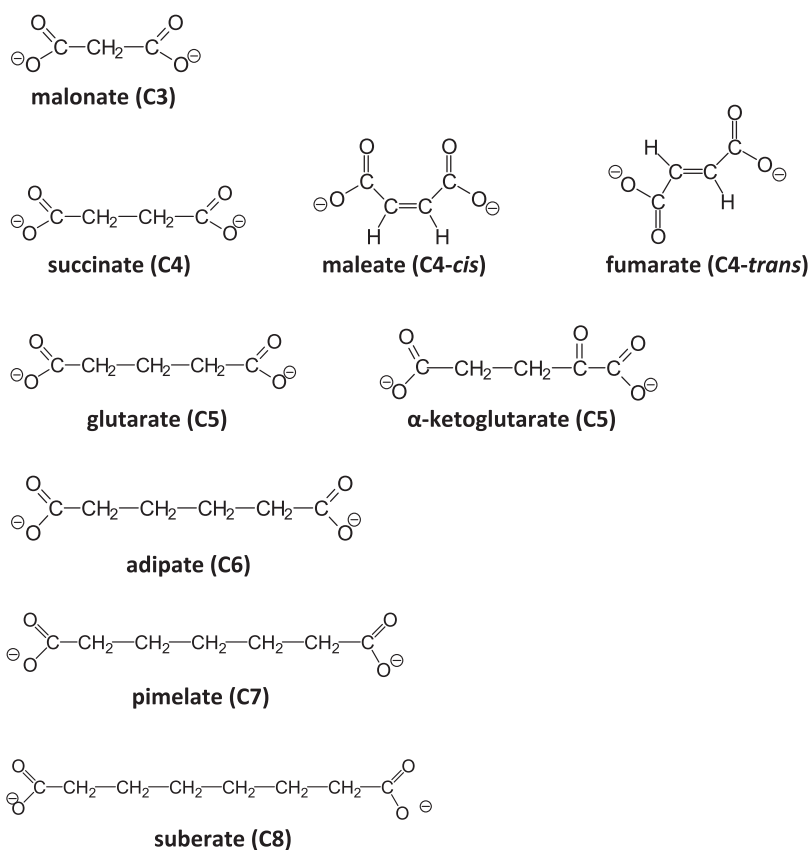


Fig. 3. Chemical structures of the dicarboxylates used in the study. The structures were designed by using the program ChemWindow, SoftShell International, Grand Junction, CO.

reflecting that dicarboxylates have in average a 13.4-fold higher affinity to OAT1 than to OAT3. Figure 7 also shows two clusters of IC_{50} values: the C4 substrates maleate, fumarate, and succinate with relatively low affinity, and the C5-C7 substrates glutarate, α -ketoglutarate, adipate, and pimelate with relatively high affinity.

DISCUSSION

Based on earlier vesicle data (25, 29), uptake of OA across the basolateral membrane of proximal tubule cells was proposed to be a tertiary active transport process. The Na^+K^+ -ATPase maintains an intracellular low-sodium concentration; the inward sodium gradient then drives three sodium ions energetically downhill and one dicarboxylate uphill through the cotransporter NaDC3 into the cells; finally, the intracellular dicarboxylates flow out downhill and drive uphill uptake of an OA through the exchangers OAT1 and OAT3. In energetic terms, one ATP is utilized per OA taken up from the blood. This arrangement of a cotransporter and one or more exchangers has been preserved during evolution from crab to human (26), suggesting some as yet not fully understood advantages.

To efficiently drive OA transport, NaDC3 must take up a dicarboxylate that can easily bind from the cell inside to OAT1 and/or OAT3 to serve as a counter anion. This task is best achieved when the affinities of all involved transporters, NaDC3, OAT1, and OAT3, are in the same range for this or these dicarboxylates to ensure proper binding and translocation. To identify such dicarboxylates, we stably expressed human NaDC3, OAT1, and OAT3 in HEK293 cells. The

affinities were checked in competition experiments by adding dicarboxylates to the incubation medium. Since all transporters were expressed in the same cell line, a direct comparison of affinities is possible. With OAT1 and OAT3, we determined the affinities to extracellular rather than to intracellular dicarboxylates, because a control of intracellular dicarboxylate concentrations is experimentally not possible. We assume, however, that the affinities of OAT1 and OAT3 to extracellular dicarboxylates are related to those at the intracellular side, at least with respect to the dicarboxylate selectivity.

For this study, human NaDC3 was stably expressed in HEK293 cells. Immunocytochemistry showed that the protein reached the plasma membrane. The two bands (~ 85 and 55 kDa) in Western blots from TCM may reflect differentially glycosylated forms, because glycanase F treatment led to the disappearance of the 85 -kDa band. Since the TCM preparation contained both plasma and intracellular membranes, the larger band may represent the fully glycosylated NaDC3 in the plasma membrane, whereas the smaller band(s) reflect unglycosylated or not completely glycosylated transporters in the endoplasmic reticulum and/or Golgi apparatus. Human NaDC3 is a protein with 11 transmembrane helices, an intracellular NH_2 and an extracellular $COOH$ terminus (2). The $COOH$ terminus carries two potential N -glycosylation sites [Asn-586, Asn-596 (38)] that are conserved in rat, mouse, and flounder NaDC3 (9, 16, 21, 31). In rabbit NaDC1, the glycosylation affected membrane targeting (23). It is likely that proper N -glycosylation serves a similar function in the human NaDC3.

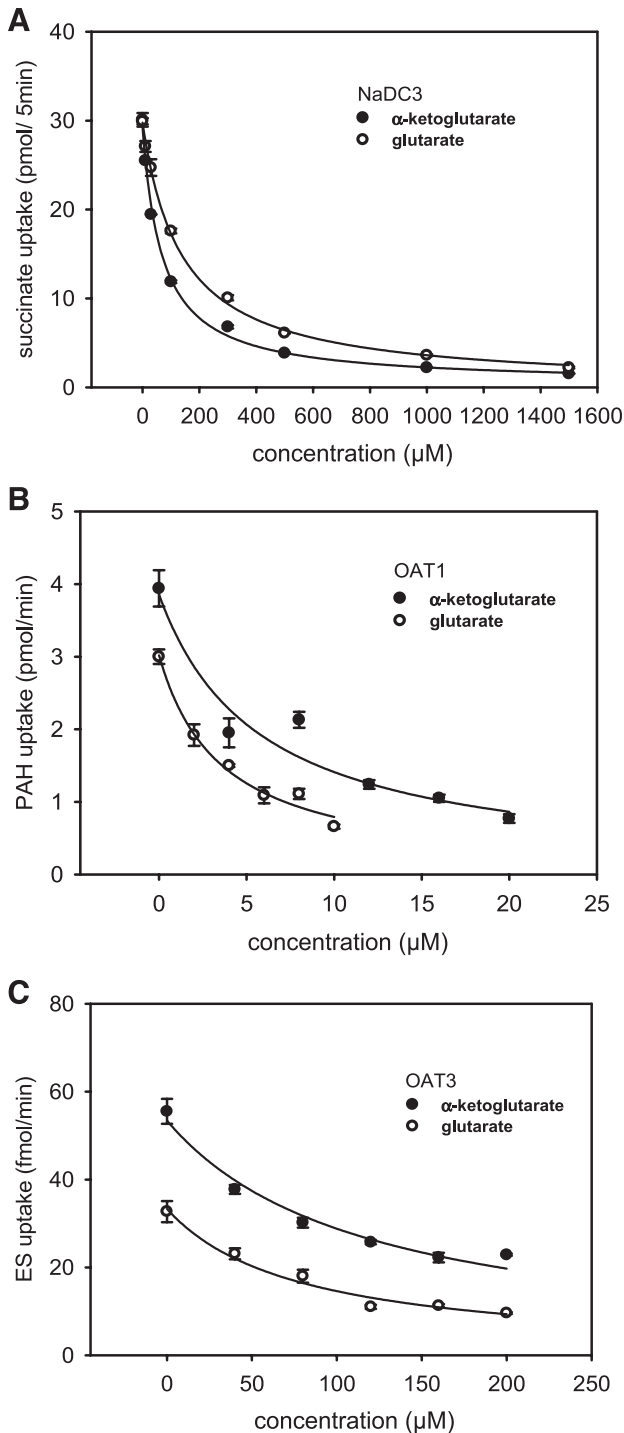


Fig. 4. Determination of the IC_{50} values for the inhibition of succinate (A), *p*-aminohippurate (PAH; B), and [3 H]estrone sulfate (ES; C) uptake by α -ketoglutarate and glutarate. A: HEK293 cells transfected with NaDC3 were incubated for 5 min with 1 μ M [14 C]succinate without or with up to 1,500 μ M α -ketoglutarate (●) or glutarate (○). B: HEK cells transfected with organic anion transporter 1 (OAT1) were incubated for 1 min with 1.1 μ M PAH without or with up to 20 μ M α -ketoglutarate (●) or up to 10 μ M glutarate (○). C: OAT3-expressing HEK cells were incubated for 1 min with 10 nM [3 H]ES without or with up to 200 μ M α -ketoglutarate (●) or glutarate (○). Each plot shows a representative experiment out of a series of 3 experiments. Uptakes in the absence of α -ketoglutarate or glutarate were not normalized and are given per well. The calculated IC_{50} values for α -ketoglutarate and glutarate in these experiments are 69.2 ± 8.2 , 137.8 ± 12.4 (A); 5.8 ± 1.2 , 3.6 ± 1.6 (B); 117.2 ± 16 , 88.0 ± 10.9 μ M (C), respectively.

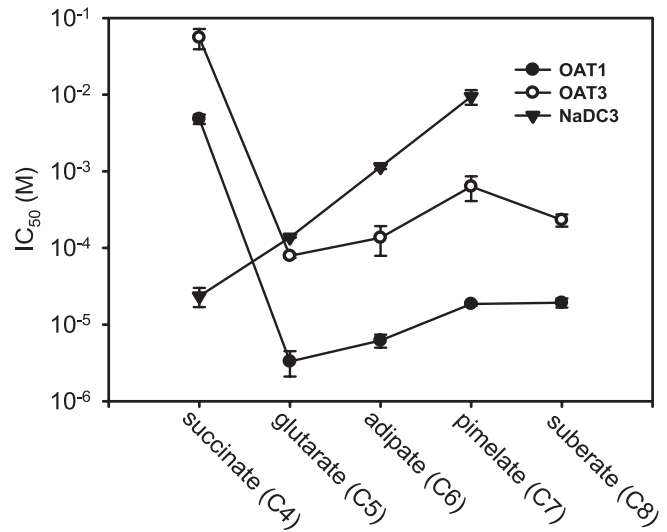


Fig. 5. Inhibitory potency of dicarboxylates of various lengths. The IC_{50} values for interaction of the dicarboxylates with NaDC3, OAT1, and OAT3 were taken from Table 1 and plotted logarithmically against the length of the dicarboxylates.

The transfected clone used in this study coded for a full-length human NaDC3 with 602 amino acids and a calculated molecular mass of 66,841 Da. However, following enzymatic deglycosylation, two bands with apparent molecular masses of

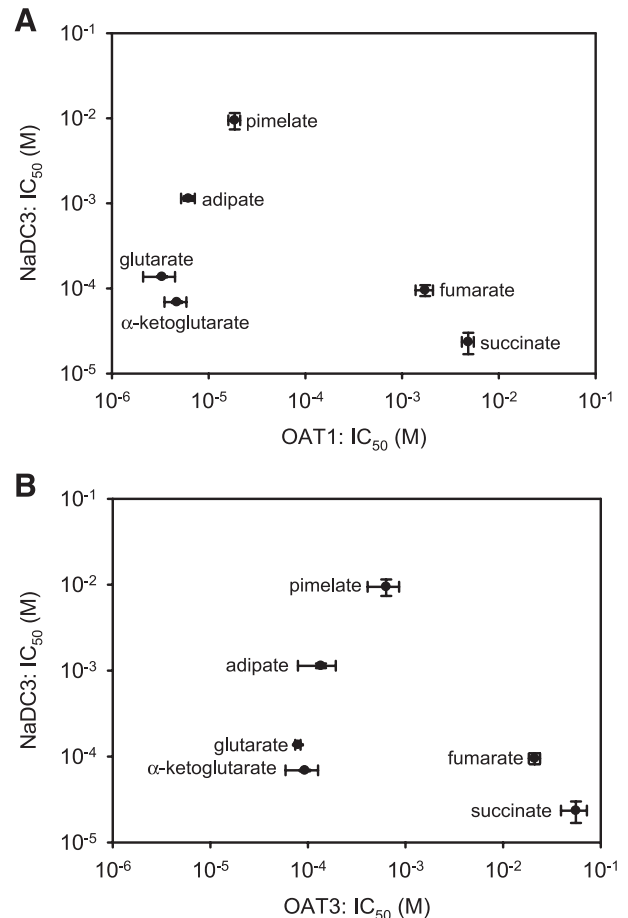


Fig. 6. Correlation between log IC_{50} at NaDC3 with those at OAT1 (A) and OAT3 (B). Data from Table 1 are replotted in a double-logarithmic scale.

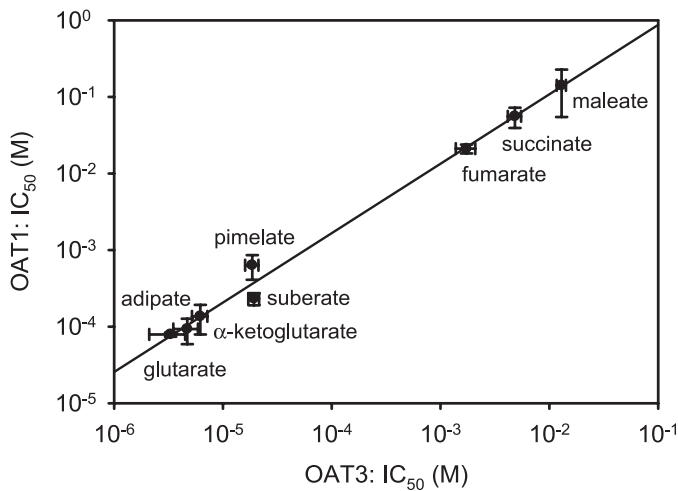


Fig. 7. Correlation of the IC₅₀ values for OAT1 and OAT3. Data are from Table 1. Linear regression was performed using SigmaPlot software.

48 and 56 kDa were obtained in Western blots. As regards the upper 56-kDa band, the deglycosylated NaDC3 may run faster in the gel than anticipated from its mass, yielding an erroneously low molecular weight. The reason for the appearance of a second band is not known. Possibly, posttranslational modification and/or limited proteolysis may account for the observation of two bands.

Stably expressed human NaDC3 showed a saturable uptake of succinate with a *K_m* of 18 μM. This figure compares favorably with determinations in other expression systems such as *Xenopus laevis* oocytes [25 μM (7)] and human retinal pigment epithelial cells [12.8 or 20.4 μM (14, 38)]. The stimulation by sodium of succinate uptake into stably transfected HEK cells was sigmoidal with a half-maximal activation effect at 44.6 mM and a Hill coefficient of 2.1, revealing a cooperative action of sodium ions on NaDC3. In another study on human NaDC3 expressed in human retinal pigment epithelial cells, activation by sodium was half-maximal at 49 mM sodium and the Hill coefficient was 2.7 (38). Taken together, NaDC3 stably expressed in HEK cells shows functional properties well in line with results on human NaDC3 in another expression system.

Using dicarboxylates of different lengths, we found that NaDC3 has the highest affinity for the four-carbons dicarboxylate succinate. Thereby, the IC₅₀ (24 μM) was very close to the *K_m* (18 μM) for succinate uptake determined with the same cells. Two other C4 dicarboxylates carrying a double bond had a lower (fumarate) or no measurable affinity (maleate), suggesting that position and distance of the carboxyl groups are critical for interaction. Likewise, the affinity decreased for longer dicarboxylates (glutarate to pimelate), indicating a strong preference of NaDC3 for saturated C4 dicarboxylates.

The five-carbon α-ketoglutarate exhibited a higher affinity than glutarate, suggesting that the α-carbonyl group facilitates binding to NaDC3. Comparable data were previously obtained with human (38) and rat (16) NaDC3, but quantitative data were so far not available.

The binding site for dicarboxylates in human NaDC3 is not known in detail. From extensive site-directed mutagenesis experiments on NaDC1, the low-affinity sodium-dicarboxylate cotransporter, it became apparent that several residues are involved in or are sensitive to dicarboxylate binding. These include, in rabbit NaDC1, Lys-84 (22), four amino acids around Ser-260 (transmembrane helix H5), Arg-349 (H7), Asp-373 (H8), Glu-475 (H9) (summarized in Ref. 20), and Ser-512 (H10) (19). Thus, it is mainly the COOH-terminal part of NaDC3 that is involved in binding and transporting dicarboxylates. Since cationic residues may bind the negatively charged dicarboxylates, we previously mutated arginines and lysines situated inside or adjacent to the putative transmembrane helices of flounder NaDC3 (13). With Lys-114 (H3) we found a residue that appeared to influence the number of sodium-binding sites. The replacement of Lys-36 by leucine (between H1 and H2) and of Lys-374 and Lys-375 by isoleucine (H8) resulted in a somewhat increased affinity for succinate; the changes were, however, not statistically significant (13), leaving open where dicarboxylates bind to NaDC3. The lack of correlation between the IC₅₀ values for dicarboxylate interaction with NaDC3 and the respective values for OAT1 or OAT3 indicates completely different molecular requirements for dicarboxylate binding.

The interaction of dicarboxylates with human OAT1 was clearly different from that of NaDC3. The affinity increased sharply from succinate to glutarate and remained high for adipate, pimelate, and suberate. The C3 dicarboxylate malonate did not inhibit OAT1. Our data are in line with an earlier qualitative study on rat OAT1 with dicarboxylates of increasing lengths inhibiting PAH uptake (34). Murine OAT1 showed the same dicarboxylate selectivity and, in a structure-activity relation approach, the charge distance turned out to be more important than hydrophobicity for the interaction of dicarboxylates with mouse OAT1 (15).

For human OAT3, we found the same sequence of potency to inhibit transport. Malonate showed no inhibition, succinate had a very low affinity, followed by a large increase in affinity for glutarate. The affinity then decreased again for larger dicarboxylates. The very high correlation between the log IC₅₀ of OAT1 and the log IC₅₀ of OAT3 strongly suggests that the structural requirements of the binding sites in these two transporters are very similar. It appears, however, that the access of dicarboxylates to the binding site of OAT3 is restricted compared with OAT1: although OAT3 had the same dicarboxylate selectivity as OAT1, the IC₅₀ values were always higher than those of OAT1.

Fig. 8. Alignment of human OAT1 and OAT3 showing conserved positively charged residues (indicated by ●) potentially involved in dicarboxylate interaction. See DISCUSSION for more information.

```

OAT1 361 QGFGVSIYLIQVIFGAVDLPARKLVGFLVINSIGRRPQMAALLLAGICILLNGVIPQDQS 420
OAT3 349 EEFVGNLYILQIIFGGVDVPAKFITILSLSYLGRHPTQAAALLLAGGAILALTFFVPLDLQ 408
OAT1 421 IVRTSLAVLGGKGLAASFNCIFLYTGELYPTMIRQTMGMGSTMARVGSIVSPLVSMTAE 480
OAT3 409 TVRTVLAVFVGGKGLSSSFSCFLYTSSELYPTVIRQTMGMVSNLWTRVGSVMVSPVLRITGE 468
    
```

Rat OAT3 was also inhibited by a series of dicarboxylates ranging from 5 to 9 carbons but IC_{50} values were not reported (1). As regards the in vivo studies in rat kidneys, succinate, glutarate, adipate, pimelate, and suberate inhibited PAH transport with K_i values of 1.35 mM, 50 μ M, 60 μ M, 350 μ M, and 350 μ M, respectively (33). With exception of succinate, the in vivo K_i values are higher than those for human OAT1 and closer to those of human OAT3. Although K_i values for rat OAT1 and OAT3 are not at hand, we assume that the in vivo data reflect a mixture of OAT1 and OAT3 with a relatively greater impact of OAT3. In support, the K_m determined for PAH uptake in vivo was 80 μ M (33), which is closer to the data reported for OAT3 than for OAT1 (6).

The binding sites for dicarboxylates in OAT1 or OAT3 are not known with certainty. Mutational analysis on the flounder OAT revealed two conserved cationic residues, Lys-394 (transmembrane helix H8) and Arg-478 (H11), as important for the interaction with dicarboxylates (39). Mutants (K395A, R478D) transported PAH but were insensitive to *cis*-inhibition and *trans*-stimulation by glutarate. The replacement of the corresponding arginine in the middle of the 11th transmembrane helix (H11) of human OAT1 (Arg-466) by neutral (R466N) or acidic residues (R466D) abolished the interaction with glutarate, whereas the replacement by the cationic lysine (R466K) preserved glutarate binding (27). These data suggested that a positive charge at position 466 is needed for binding and/or transport of dicarboxylates by human OAT1. In a three-dimensional homology model, human OAT1 showed a large cavity open to the intracellular side with Arg-466 positioned right at the opening of the putative binding pocket (24). The model located another cationic residue, Lys-431 in H10, close to the binding pocket. Mutation of this residue inactivated OAT1 (24), whereas, in human OAT3, the replacement of the corresponding Lys-419 abolished interaction with glutarate (summarized in Ref. 30). Taken together, it appears that basic amino acid residues in *trans*-membrane helices 8, 10, and 11 play a role in dicarboxylate binding. In human OAT1, these residues are Lys-382 (H8), Lys-431 (H10), and Arg-466 (H11). The corresponding residues in human OAT3 are Lys-370 (H8), Lys-419 (H10), and Arg-454 (H11). At the level of the primary structure, these cationic amino acids have exactly the same distance to each other (see Fig. 8). Therefore, these residues may be situated at equivalent places in the three-dimensional transporter, explaining why the dicarboxylate specificity of OAT1 and OAT3 correlates highly as found in this study. The generally higher affinity of OAT1 may be due to a better accessibility of dicarboxylates to the binding site that is otherwise similar between OAT1 and OAT3.

As regards the functional coupling between NaDC3 and OAT1/OAT3, succinate and glutarate appear not ideal. Succinate has a high affinity for NaDC3 but very low affinities for OAT1 and OAT3. Thus, succinate, intracellularly accumulated by NaDC3, may not serve as a proper counterion for PAH and ES uptake through OAT1 and OAT3. Although glutarate has a relatively high affinity for all transporters, its plasma concentration (0.6–2.9 μ M) (4) is low, probably leading to an inefficient intracellular accumulation of this dicarboxylate by NaDC3. Our results provide quantitative evidence for α -ketoglutarate being ideal for the functional coupling of NaDC3 with OAT1 and OAT3 for three reasons. First, its plasma concentration (8.6 μ M) (28) is higher than

that of glutarate. Second, NaDC3 has a higher affinity for α -ketoglutarate than glutarate. Thus, NaDC3 most probably transports more α -ketoglutarate than glutarate into the proximal tubule cell. Third, OAT1 and OAT3 have relatively high affinities for C5 dicarboxylates, enabling them to exchange intracellular α -ketoglutarate against PAH, ES, and other endogenous and exogenous OA.

GRANTS

This study was supported by a grant from the Deutsche Forschungsgemeinschaft to B. C. Burckhardt (BU 998/5-1) and a grant from the Ministry of Science, Education, and Sports, Republic of Croatia to I. Sabolic (0022-0222148-2146).

We dedicate this publication to the late Prof. Dr. K. J. Ullrich, a pioneer in the field of renal organic anion transport.

DISCLOSURES

No conflicts of interest, financial or otherwise, are declared by the author(s).

REFERENCES

1. Anzai N, Jutabha P, Enomoto A, Yokoyama H, Nonoguchi H, Hirata T, Shiraya K, He X, Cha SH, Takeda M, Miyazaki H, Sakata T, Tomita K, Igarashi T, Kanai Y, Endou H. Functional characterization of rat organic anion transporter 5 (*Slc22a19*) at the apical membrane of renal proximal tubules. *J Pharmacol Exp Ther* 315: 534–544, 2005.
2. Bai XY, Chen X, Sun AQ, Feng Z, Hou K, Fu B. Membrane topology structure of human high-affinity, sodium-dependent dicarboxylate transporter. *FASEB J* 21: 2409–2417, 2007.
3. Bakhiya N, Stephani M, Bahn A, Ugele B, Seidel A, Burckhardt G, Glatt H. Uptake of chemically reactive, DNA-damaging sulfuric acid esters into renal cells by human organic anion transporters. *J Am Soc Nephrol* 17: 1414–1421, 2006.
4. Baric I, Wagner L, Feyh P, Liesert M, Buckel W, Hoffmann GF. Sensitivity and specificity of free and total glutaric acid and 3-hydroxyglutaric acid measurements by stable-isotope dilution assays for the diagnosis of glutaric aciduria type I. *J Inher Metab Dis* 22: 867–882, 1999.
5. Bradford MM. A rapid and sensitive method for the quantitation of microgram quantities of protein utilizing the principle of protein-dye binding. *Anal Biochem* 72: 248–254, 1976.
6. Burckhardt BC, Burckhardt G. Transport of organic anions across the basolateral membrane of proximal tubule cells. *Rev Physiol Biochem Pharmacol* 146: 95–158, 2003.
7. Burckhardt BC, Lorenz J, Kobbe C, Burckhardt G. Substrate specificity of the human renal sodium dicarboxylate cotransporter, hNaDC-3, under voltage-clamp conditions. *Am J Physiol Renal Physiol* 288: F792–F799, 2005.
8. Burckhardt G, Burckhardt BC. In vitro and in vivo evidence of the importance of organic anion transporters (OATs) in drug therapy. In: *Drug Transporters*, edited by Fromm MF and Kim RB. Heidelberg, Germany: Springer-Verlag, 2011.
9. Chen XM, Tsukaguchi H, Chen XZ, Berger UV, Hediger MA. Molecular and functional analysis of SDC2T, a novel rat sodium-dependent dicarboxylate transporter. *J Clin Invest* 103: 1159–1168, 1999.
10. Cihlar T, Ho ES. Fluorescence-based assay for the interaction of small molecules with the human renal organic anion transporter 1. *Anal Biochem* 283: 49–55, 2000.
11. De Lean A, Munson PJ, Rodbard D. Simultaneous analysis of families of sigmoidal curves: application to bioassay, radioligands assay, and physiological dose-response curves. *Am J Physiol Endocrinol Metab Gastrointest Physiol* 235: E97–E102, 1978.
12. Eraly SA, Vallon V, Rieg T, Gangotti JA, Wikoff WR, Siuzdak G, Barshop BA, Nigam SK. Multiple organic anion transporters contribute to net renal excretion of uric acid. *Physiol Genomics* 33: 180–192, 2008.
13. Hagos Y, Steffgen J, Rizwan AN, Langheit D, Knoll A, Burckhardt G, Burckhardt BC. Functional roles of the cationic amino acid residues in the sodium-dicarboxylate cotransporter 3 (NaDC-3) from winter flounder. *Am J Physiol Renal Physiol* 291: F1224–F1231, 2006.
14. Huang W, Wang H, Kekuda R, Fei YJ, Friedrich A, Wang J, Conway SJ, Cameron RS, Leibach FH, Ganapathy V. Transport of *N*-acetylaspargate by the Na⁺-dependent high-affinity dicarboxylate transporter

- NaDC3 and its relevance to the expression of the transporter in the brain. *J Pharmacol Exp Ther* 295: 392–403, 2000.
15. **Kaler G, Truong DM, Khandelwal A, Nagle M, Eraly SA, Swaan PW, Nigam SK.** Structural variation governs substrate specificity for organic anion transporter (OAT) homologs. Potential remote sensing by OAT family members. *J Biol Chem* 282: 23841–23853, 2007.
 16. **Kekuda R, Wang H, Huang W, Pajor AM, Leibach FH, Devoe LD, Prasad PD, Ganapathy V.** Primary structure and functional characteristics of a mammalian sodium-coupled high affinity dicarboxylate transporter. *J Biol Chem* 274: 3422–3429, 1999.
 17. **Kimura T, Perry J, Anzai N, Pritchard JB, Moaddel R.** Development and characterization of immobilized human organic anion transporter based liquid chromatography stationary phase: hOAT1 and hOAT2. *J Chromatogr* 15: 267–271, 2007.
 18. **Ljubojevic M, Balen D, Breljak D, Kusan M, Anzai N, Bahn A, Burckhardt G, Sabolic I.** Renal expression of organic anion transporter OAT2 in rats and mice is regulated by sex hormones. *Am J Physiol Renal Physiol* 292: F361–F372, 2007.
 19. **Oshiro N, Pajor AM.** Ala-504 is a determinant of substrate binding affinity in the mouse Na⁺/dicarboxylate cotransporter. *Biochim Biophys Acta* 1758: 781–788, 2006.
 20. **Pajor AM.** Molecular properties of the SCL13 family of dicarboxylate and sulfate transporters. *Pflügers Arch* 451: 597–605, 2006.
 21. **Pajor AM, Gangula R, Yao X.** Cloning and functional characterization of a high-affinity Na⁺/dicarboxylate cotransporter from mouse brain. *Am J Physiol Cell Physiol* 280: C1215–C1223, 2001.
 22. **Pajor AM, Kahn ES, Gangula R.** Role of cationic amino acids in the Na⁺/dicarboxylate cotransporter NaDC-1. *Biochem J* 350: 677–683, 2000.
 23. **Pajor AM, Sun N.** Characterization of the rabbit renal Na⁺/dicarboxylate cotransporter using antifusion protein antibodies. *Am J Physiol Cell Physiol* 271: C1808–C1816, 1996.
 24. **Perry JL, Dembla-Rajpal N, Hall LA, Pritchard JB.** A three-dimensional model of human organic anion transporter 1. Aromatic amino acids required for substrate transport. *J Biol Chem* 281: 38071–38079, 2006.
 25. **Pritchard JB.** Coupled transport of *p*-aminohippurate by rat kidney basolateral membrane vesicles. *Am J Physiol Renal Fluid Electrolyte Physiol* 255: F597–F604, 1988.
 26. **Pritchard JB, Miller DS.** Mechanisms mediating renal secretion of organic anions and cations. *Physiol Rev* 73: 765–796, 1993.
 27. **Rizwan AN, Krick W, Burckhardt G.** The chloride dependence of the human organic anion transporter 1 (hOAT1) is blunted by mutation of a single amino acid. *J Biol Chem* 282: 13402–13409, 2007.
 28. **Rocchiccioli F, Leroux JP, Cartier PH.** Microdetermination of 2-ketoglutaric acid in plasma and cerebrospinal fluid by capillary gas chromatography mass spectrometry: application to pediatrics. *Biomed Mass Spectrom* 11: 24–28, 1984.
 29. **Shimada H, Moewes B, Burckhardt G.** Indirect coupling to Na⁺ of *p*-aminohippuric acid uptake into rat renal basolateral membrane vesicles. *Am J Physiol Renal Fluid Electrolyte Physiol* 253: F795–F801, 1987.
 30. **Srimaroeng C, Perry JL, Pritchard JB.** Physiology, structure, and regulation of the cloned organic anion transporters. *Xenobiotica* 38: 889–935, 2008.
 31. **Steffgen J, Burckhardt BC, Langenberg C, Kühne L, Müller GA, Burckhardt G, Wolff NA.** Expression cloning and characterization of a novel sodium-dicarboxylate cotransporter from winter flounder kidney. *J Biol Chem* 274: 20191–20196, 1999.
 32. **Sweet DH, Miller DS, Pritchard JB, Fujiwara Y, Beier DR, Nigam SK.** Impaired organic anion transport in kidney and choroid plexus of organic anion transporter 3 [*Oat3* (*Slc22a8*)] knockout mice. *J Biol Chem* 277: 26934–26943, 2002.
 33. **Ullrich KJ, Rumrich G, Fritsch G, Klöss S.** Contraluminal para-aminohippurate (PAH) transport in the proximal tubule of the rat kidney. II. Specificity: aliphatic dicarboxylic acids. *Pflügers Arch* 408: 38–45, 1987.
 34. **Uwai Y, Okuda M, Takami K, Hashimoto Y, Inui KI.** Functional characterization of the rat multispecific organic anion transporter OAT1 mediating basolateral uptake of anionic drugs in the kidney. *FEBS Lett* 438: 321–324, 1998.
 35. **Vallon V, Rieg T, Ahn SY, Wu W, Eraly SA, Nigam SK.** Overlapping in vitro and in vivo specificities of the organic anion transporters OAT1 and OAT3 for loop and thiazide diuretics. *Am J Physiol Renal Physiol* 294: F867–F873, 2008.
 36. **VanWert AL, Gionfriddo MR, Sweet DH.** Organic anion transporters: discovery, pharmacology, regulation and roles in pathophysiology. *Biopharm Drug Dispos* 31: 1–71, 2010.
 37. **VanWert AL, Srimaroeng C, Sweet DH.** Organic anion transporter 3 (*Oat3/Slc22a8*) interacts with carboxyfluoroquinolones, and deletion increases systemic exposure to ciprofloxacin. *Mol Pharmacol* 74: 122–131, 2008.
 38. **Wang H, Fei YJ, Kekuda R, Yang-Feng TL, Devoe LD, Leibach FH, Prasad PD, Ganapathy V.** Structure, function, and genomic organization of human Na⁺-dependent high-affinity dicarboxylate transporter. *Am J Physiol Cell Physiol* 278: C1019–C1030, 2000.
 39. **Wolff NA, Grünwald B, Friedrich B, Lang F, Godehardt S, Burckhardt G.** Cationic amino acids involved in dicarboxylate binding of the flounder renal organic anion transporter. *J Am Soc Nephrol* 12: 2012–2018, 2001.